A00-45055

2000-01-5593

Optimal and Near-Optimal Take-off Maneuvers in the Presence of Windshear

K. Elferink and H. G. Visser
Delft University of Technology, The Netherlands

2000 World Aviation Conference
October 10-12, 2000
San Diego, CA

SAE The Engineering Society For Advancing Mobility Land Sea Air and Space® INTERNATIONAL

SAE International
400 Commonwealth Drive
Warrendale, PA 15096-0001 U.S.A.

AIAA
American Institute of Aeronautics and Astronautics
370 L'Enfant Promenade, S.W.
Washington, D.C. 20024

Published by the American Institute of Aeronautics and Astronautics (AIAA) at 1801 Alexander Bell Drive, Suite 500, Reston, VA 22091 U.S.A., and the Society of Automotive Engineers (SAE) at 400 Commonwealth Drive, Warrendale, PA 15096 U.S.A.

Produced in the U.S.A. Non-U.S. purchasers are responsible for payment of any taxes required by their governments.

ISSN #0148-7191

All AIAA papers are abstracted and indexed in International Aerospace Abstracts and Aerospace Database.

All SAE papers, standards and selected books are abstracted and indexed in the Global Mobility Database.

Copies of this paper may be purchased from:

AIAA's document delivery service
Aeroplus Dispatch
1722 Gilbreth Road
Burlingame, California 94010-1305
Phone: (800) 662-2376 or (415) 259-6011
Fax: (415) 259-6047

or from:

SAExpress Global Document Service
c/o SAE Customer Sales and Satisfaction
400 Commonwealth Drive
Warrendale, PA 15096
Phone: (724) 776-4970
Fax: (724) 776-0790

SAE routinely stocks printed papers for a period of three years following date of publication. Quantity reprint rates are available.

2000-01-5593

Optimal and Near-Optimal Take-off Maneuvers in the Presence of Windshear

K. Elferink and H.G. Visser
Delft University of Technology, The Netherlands

ABSTRACT

This paper is concerned with the development of short-range forward-look guidance strategies for take-off maneuvers in the presence of windshear, with reference to flight in the vertical and horizontal plane. In addition to the horizontal shear, the presence of a downdraft is assumed. First, two open-loop optimal escape strategies are considered, viz. a performance maintaining strategy and a survival strategy, where it is assumed that the windshear is detected in an early stage of the encounter. Next, two closed-loop guidance strategies featuring short-range forward-look detection, which closely approximate the open-loop optimal solutions, are developed. Numerical results show that lateral maneuvering, in which an aircraft is turned away from the microburst, improves the flight performance significantly in both optimal escape strategies. The simulation results demonstrate that the employed closed-loop guidance strategies are able to closely approximate the open-loop optimal trajectories, in both longitudinal and lateral escape maneuvers.

INTRODUCTION

Weather phenomena that cause windshear, especially the so-called microburst present a significant safety hazard during the take-off and landing. A microburst is a strong downdraft that occurs when a column of air at high altitude quickly cools and rapidly descends to the ground. Upon nearing the ground, the downward moving air spreads out horizontally in all directions. The radially divergent winds subsequently evolve in one or more circular vortices, encircling the downflow.

An aircraft that penetrates the center of a microburst will initially experience an increasing headwind, which increases the aircraft's performance. As the aircraft proceeds the downdraft increases and the headwind shifts into a tailwind, causing the aircraft to lose energy. This energy drain may be sufficiently strong to prevent the aircraft from recovering, see figure 1.

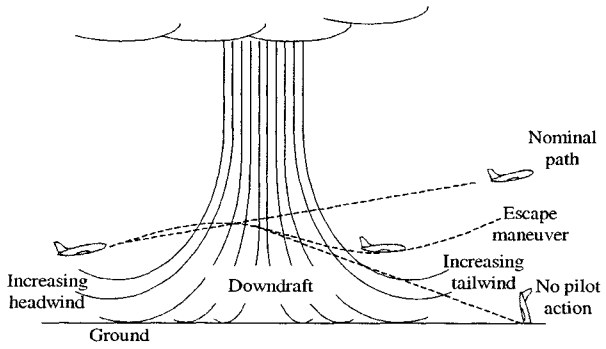

Fig. 1: Microburst encounter during take-off.

Currently, reactive windshear warning systems are being installed aboard aircraft, which are able to detect such potentially dangerous situations as described above and to alert the pilot once the microburst is encountered so that appropriate actions can be taken. Even better than reactive systems, early detection and warning of hazardous windshear can significantly increase the survivability during take-off and landing. Therefore, substantial research efforts are currently undertaken to develop so-called forward-look windshear detection systems. Forward-look detection systems can be divided in short-range (e.g. Doppler LIDAR [1]) and long-range (e.g. Microwave Doppler Radar [1]) forward-look detection systems. However, in view of the high cost of long-range forward-look detection systems, it seems questionable whether such systems should be mandated for e.g. light regional aircraft (FAR 23). In this paper only short-range forward-look detection systems will be considered.

Short-range forward-look systems scan the departure or approach path to determine the spatial extent of the affected area and relate this to an estimate of airplane

exposure based on the current state (notably, airspeed). The advance warning provided by a forward-look system allows the pilot to build-up an energy buffer in the form of an airspeed reserve just a few seconds before the actual penetration of the microburst. It must be taken into account that these short-range forward-look detection systems are defined as systems having a total detection range less than the microburst diameter. Therefore these systems are only able to provide local wind information. As a consequence, the development of appropriate windshear escape guidance strategies for take-off and landing maneuvers remains necessary.

Obviously, the most desirable guidance is one that ensures flight on an *optimal* escape trajectory. However, the calculation of an optimal trajectory is based on the assumption of perfect global wind information, but as mentioned before, in the real-world sensors are only able to provide local information of the wind flow field with a fair degree of uncertainty. Thus, in reality it is almost impossible to create an optimal trajectory.

In the present study at first open-loop optimal take-off trajectories are calculated using two different escape strategies. As an extension to previous open-loop optimization studies [2, 3, 4], it is assumed that the microburst is detected in an early stage of the encounter. This offers the possibility of applying escape procedures involving lateral maneuvering (see [5]). Subsequently the obtained open-loop optimal solutions are used to develop onboard closed-loop guidance strategies for the take-off maneuver, which make use of short-range forward-look windshear detection systems in order to closely approximate the open-loop optimal trajectories.

MODELING OF MICROBURST ENCOUNTER

EQUATIONS OF MOTION. A point-mass model of an aircraft, as defined in [5], describing the aircraft's dynamics under windshear conditions, is used to analyze the airplane's performance during a microburst encounter. The set of equations of motion embodies the following assumptions: (1) a steady wind flow field; (2) a zero angle-of sideslip; and (3) a constant aircraft weight.

Using a wind-axes reference frame, the set of equations of motion in a three-dimensional space can be written as:

$$\dot{x} = V\cos\gamma\cos\chi + W_x \tag{1}$$

$$\dot{y} = V\cos\gamma\sin\chi + W_y \tag{2}$$

$$\dot{h} = V\cos\gamma + W_h \tag{3}$$

$$\dot{E} = \frac{\left\{T\left[1-\frac{1}{2}(\alpha+\delta)^2\right]-D\right\}V}{W} + W_h - \frac{V}{g}\left(\dot{W}_x\cos\gamma\cos\chi + \dot{W}_y\cos\gamma\sin\chi + \dot{W}_h\sin\gamma\right) \tag{4}$$

$$\dot{\gamma} = \frac{g}{V}\left(\frac{L+T(\alpha+\delta)}{W}\cos\mu - \cos\gamma\right) - \frac{1}{V}\left(\dot{W}_x\sin\gamma\cos\chi + \dot{W}_y\sin\gamma\sin\chi - \dot{W}_h\cos\gamma\right) \tag{5}$$

$$\dot{\chi} = \frac{g}{V\cos\gamma}\left(\frac{L+T(\alpha+\delta)}{W}\sin\mu\right) + \frac{1}{V\cos\gamma}\left(\dot{W}_x\sin\chi - \dot{W}_y\cos\chi\right) \tag{6}$$

where x, y and h are the position coordinates; E is the specific energy; γ is the flight path angle; and χ is the heading angle. W_x, W_y and W_h are the three components of the wind vector. The thrust T is assumed to have a fixed inclination δ relative to the zero-lift axis. To simplify the optimal control analysis, a small-angle approximation has been employed in the equations of motion for the thrust components along and perpendicular to the airspeed vector respectively, i.e., $\cos(\alpha+\delta) \approx 1-\frac{1}{2}(\alpha+\delta)^2$ and $\sin(\alpha+\delta) \approx (\alpha+\delta)$.

Here, specific energy E is used as a state variable instead of the airspeed V to provide a better insight in the impact of windshear on airplane performance. The specific energy can be defined as the sum of the air-mass relative kinetic energy and the inertial potential energy. The airspeed should be regarded as a function of energy and altitude and can be obtained from the relation:

$$V = \sqrt{(E-h)2g} \tag{7}$$

In the mathematical model the controls are (1) the bank angle μ, which is constrained by:

$$|\mu| = \mu_{\max} \tag{8}$$

and (2) the angle of attack α, which has to remain within the range:

$$0 \le \alpha \le \alpha_{\max} \tag{9}$$

For the present study the rate of change of the control variables α and μ is assumed to be unlimited. This implies that an instantaneous change in angle of attack or bank angle is possible.

Lift and drag are modeled as a function of the angle of attack, the airspeed and the altitude, with the following definitions:

$$L = C_L(\alpha)\tfrac{1}{2}\rho V^2 S, \qquad D = C_D(\alpha)\tfrac{1}{2}\rho V^2 S \tag{10}$$

AERODYNAMIC AND THRUST CHARACTERISTICS. For the present study a point-mass model of a Boeing 727 with three JT8D turbofan engines has been used, which is adapted from a model originally developed by Miele et al. [2]. The main characteristics of this aircraft model are:

$$T = T_0 + T_1 V + T_2 V^2 \tag{11}$$

$$C_L(\alpha) = L_0 + L_1 \alpha, \qquad 0 \le \alpha \le \alpha_{ref} \tag{12}$$

$$C_L(\alpha) = L_0 + L_1 \alpha + L_2 (\alpha - \alpha_{ref})^2, \quad \alpha_{ref} \le \alpha \le \alpha_{\max} \tag{13}$$

$$C_D(\alpha) = D_0 + D_1 \alpha + D_2 \alpha^2 \tag{14}$$

The values of these coefficients for the aircraft in take-off configuration can be found in [3] and [6].

MICROBURST WIND MODEL. To quantify the described microburst phenomena, an analytical model is applied that is used by Visser in open-loop optimization studies [5] and is an axisymmetric three-dimensional extension of the two-dimensional model presented in [6]. The analytical axisymmetric representation of a microburst model has the mathematical advantage that it is a very smooth approximation of a microburst flowfield, so it is very suitable for application in optimal control problems.

Because of the axisymmetric character of the microburst model, it is convenient to use polar coordinates to describe the flowfield in a horizontal plane (see Fig. 2). The induced radial and vertical wind velocities can be computed through the following relations:

$$W_r = f_r \left(\frac{100}{\left[\frac{r - D/2}{200}\right]^2 + 10} - \frac{100}{\left[\frac{r + D/2}{200}\right]^2 + 10} \right) \tag{15}$$

$$W_h = -f_h \left(\frac{0.4h}{\left(\frac{r}{400}\right)^4 + 10} \right) \tag{16}$$

In Eqs. (15) and (16) r can be defined as the radial distance from the microburst center located at point (x_c, y_c):

$$r = \sqrt{(x - x_c)^2 + (y - y_c)^2} \tag{17}$$

Using polar coordinates, the horizontal wind components W_x and W_y can be related to the radial wind velocity W_r:

$$W_x = \cos\chi_W W_r(r) \tag{18}$$

$$W_y = \sin\chi_W W_r(r) \tag{19}$$

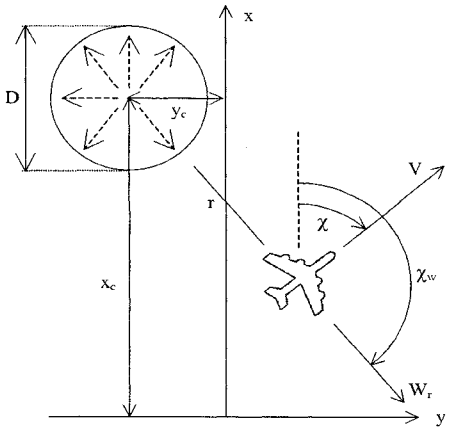

Figure 2: Geometry of microburst encounter

The microburst velocity profiles can be shaped by the windshear intensity parameters f_r and f_h, and the parameter D, wich specifies the diameter of the peak radial outflow velocity contour. In this study D is always taken as 2000 m and the parameters f_r and f_h are set equal to 2.

WINDSHEAR HAZARD FACTOR. The windshear hazard factor, or F-factor, is an important characteristic parameter, used in the evaluation of aircraft performance in microburst windfields. The windshear hazard factor can be defined as [5, 7]:

$$F \doteq \frac{T\cos(\alpha + \delta) - D}{W} - \frac{\dot{E}}{V} \tag{20}$$

Physically the windshear hazard factor can be interpreted as the loss or gain in available excess thrust-to-weight ratio due to the combined effect of downdraft and horizontal windshear. Substitution of Eq. (4) into Eq. (20) results in the following expression for the F-factor:

$$F = \frac{1}{g}\left(\dot{W}_x \cos\gamma\cos\chi + \dot{W}_y \cos\gamma\sin\chi + \dot{W}_h \sin\gamma\right) - \frac{W_h}{V} \tag{21}$$

Eq. (21) shows that the F-factor does not merely depend on the spatial location of the aircraft within the flow field, but rather on all state variables.

OPEN-LOOP OPTIMAL TRAJECTORIES

PROBLEM FORMULATION. To avert an impending crash, two possible objectives are considered. The first objective is to maintain the nominal (windless) flight path as closely as possible without stall and is therefore called a performance maintaining strategy. Since altitude is a direct concern, climb rate is used to represent this strategy. This problem can be formulated as the minimization of the peak value of the difference between a reference climb rate, assumed constant, and the actual climb rate at any point along the trajectory:

$$J^* = \min J = \min\left[\max_t\left(\dot{h}_{ref} - \dot{h}(t)\right)\right], \quad 0 \le t \le t_f \tag{22}$$

This minimax criterion, or Chebyshev performance index, can be approximated by a Bolza performance index, using the following transformation [7]:

$$\lim_{k\to\infty}\left[\int_0^{t_f}\left(\dot{h}_{ref} - \dot{h}(t)\right)^{2k} dt\right]^{\frac{1}{2k}} = \max_t\left(\dot{h}_{ref} - \dot{h}(t)\right) \tag{23}$$

The Bolza performance index can now be defined as:

$$J^* = \min J = \min\int_0^{t_f}\left(\dot{h}_{ref} - \dot{h}\right)^q dt \tag{24}$$

for large values of the positive, even exponent q. The numerical values of the constants in Eq.(24) that have been used here are $q = 6$ and $\dot{h}_{ref} = 12$ m/s.

The second objective on the other hand, is to seek the longest possible stay in the air. In this so-called survival strategy the specific energy is used to represent the aircraft's potential to survive longer. The problem is to maximize the minimum specific energy occurring at any point along the trajectory. This problem can equivalently be formulated as the minimization of the peak value of the difference between a reference specific energy, assumed constant, and the actual specific energy at any point along the trajectory:

$$J^* = \min J = \min\left[\max_t\left(E_{ref} - E(t)\right)\right], \quad 0 \le t \le t_f \tag{25}$$

Using Eq. (23), this Chebyshev performance index can be approximated by the following Bolza performance index:

$$J^* = \min J = \min\int_0^{t_f}\left(E_{ref} - E\right)^q dt \tag{26}$$

for large values of the positive, even exponent q. The numerical values of the constants in Eq.(26) that have been used here are $q = 6$ and E_{ref} =1200 m.

Because the specific energy is defined as the sum of the air-mass relative kinetic energy and the inertial potential energy, it is important to realize that any attempt to increase the specific energy at termination of the encounter typically comes at the expense of a lower recovery altitude. Similar to the maximum final energy (longitudinal) analysis presented in [2], this is the reason for including a minimum safe altitude constraint (h_{min}) in this strategy.

BOUNDARY CONDITIONS. All state variables are prescribed at the initial value of time at which the escape maneuver is commenced. These initial conditions represent the situation in which the aircraft would fly a safe climb out. The following initial conditions are used:

$x_0 = 0$ m; $y_0 = 0$ m; $h_0 = 91.44$ m;

$E_0 = 454.37$ m; $V_0 = 84.37$ m/s;

$\gamma_0 = 7$ °; $\chi_0 = 0$ °;

No terminal boundary conditions on the state variables have been imposed.

NUMERICAL METHOD. To solve the preceding problems, a direct trajectory optimization method that represents state and control variables by piecewise polynomials is used. The employed optimization method is based, on the nonlinear programming and collocation method introduced by Hargraves and Paris [8].

NUMERICAL RESULTS. Longitudinal escape maneuvers. To study the characteristic features of the two proposed escape strategies, straight flights along the x-axis, right through the center of the microburst, are considered. The results are presented in Fig. 3.

In this scenario, the center of the microburst is located on the runway centerline extension, at 1500 m from the startingpoint of the optimization. The minimum altitude constraint is taken to be h_{min} = 60.96 m (= 200 ft). Since it is assumed that the aircraft is in the initial stage of a climb out, maximum thrust is used. This implies that the angle of attack α is the only control.

It is noted that for the considered microburst size and location, the aircraft position at which the escape is commenced is just outside the maximum radial outflow velocity contour. From an operational perspective, the assumed scenario is therefore representative of an

encounter featuring short-range forward-look windshear detection. This makes it possible to compare the optimal open-loop solutions with the developed closed-loop forward-look guidance techniques, which will be discussed later.

Figure 3a. shows the time history for the flight altitude. It can be seen that the survival strategy descends to, and remains a long period, at the minimum altitude in order to gain airspeed (Fig. 3c.) and to avoid large downdrafts. Even when the downburst becomes favorable again (negative F-factors), the aircraft doesn't start to climb directly. During the $h = h_{min}$ arc, the angle of attack increases to cope with the decreasing airspeed caused by the change from headwind to tailwind coupled with downdraft, but in general the angle of attack is low and never reaches the stick-shaker limit α_{max} (see Fig. 3d.).

The performance strategy, on the other hand, keeps a certain climb rate at the expense of airspeed loss. Towards

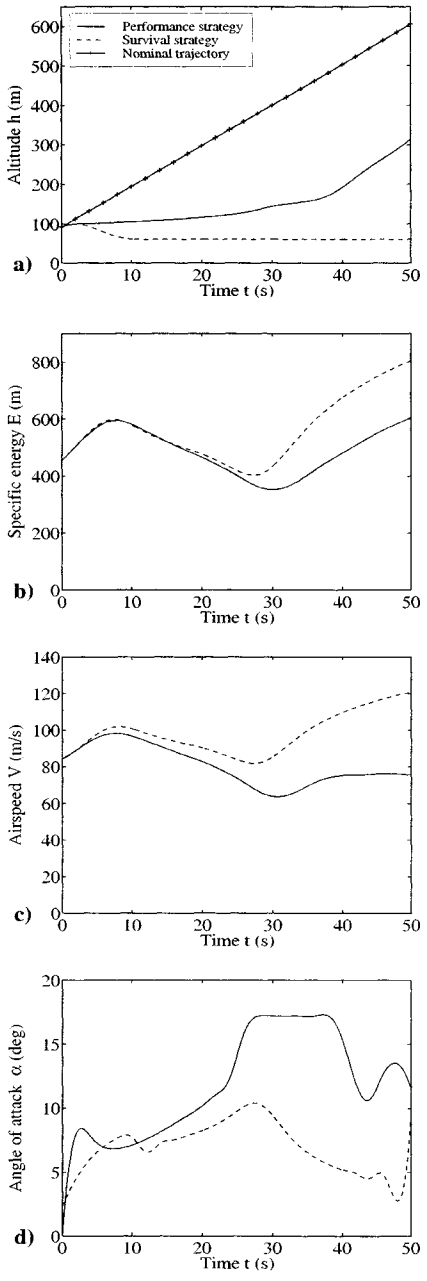

the end of the encounter the nominal climb rate is gradually restored. However, the aircraft has to fly at the maximum angle of attack for a long time in order to keep the altitude as close as possible to the intended flight path. This results in a phugoid type of flight. In general maximum angle of attack, and consequently minimum airspeed, is reached at the end of the high shear region. During the first 8 seconds of the microburst encounter the specific energy increases for both strategies as a result of the increasing headwind (Fig. 3b.). Since the specific energy is defined as the sum of kinetic and potential energy, the increasing specific energy is mainly a result of increasing the kinetic level (gain airspeed). This indicates that it is more effective to increase energy by increasing airspeed. Due to the higher climb rate at the beginning, the performance strategy experiences a higher downdraft during the unfavorable wind region. Together with the high values of the horizontal shear velocities in this region this results in a low specific energy level in comparison with the survival strategy.

To evaluate which of the two escape strategies is the safest strategy, the windshear intensity parameters (see Eqs. (15) and (16)) are varied. Fig. 4. shows that in a very severe microburst environment the aircraft in a performance maintaining strategy also tends to descend to low flight altitudes. This implies that the performance

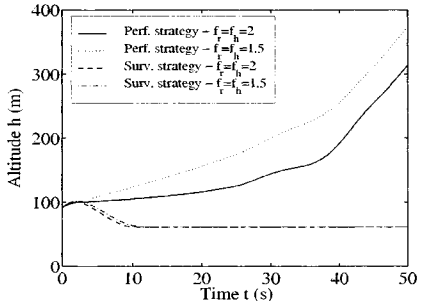

Fig. 4 Comparison of optimal solutions for various windshear intensity parameters. Longitudinal maneuvering.

maintaining strategy in a severe microburst environment eventually evolves into a survival strategy. Since in reality the intensity of a microburst is difficult to assess for an aircraft equipped with a short-range windshear detection system, initiation of a survival strategy in a mild microburst environment will lead to very high airspeeds at the minimum altitude constraint $h = h_{min}$. This indicates that the performance maintaining strategy is probably the safest strategy.

Lateral escape maneuvers. Most of previous studies [3, 4] on aircraft escape maneuvers during microburst encounters have assumed that penetrating the microburst center in straight flight is the only possible choice for a pilot to survive. However, if the altitude at which the windshear

warning is received is sufficiently high, a lateral escape maneuver which turns the aircraft away from the microburst center may result in better flight performance (see [5, 7]).

In the present section lateral escape maneuvers are applied in the take-off phase to study the effects of banking on aircraft's survivability. The same scenario as used in the previous section is considered, only now a maximum bank angle of 15° is allowed. The results are illustrated in Fig. 5.

Figure 5a shows the flight altitudes for the lateral escape maneuvers for the two escape strategies. It can be seen that a turn in the horizontal plane causes an improved climb performance during the performance strategy and makes it possible to leave the maximum angle of attack earlier (Fig. 5d). During the survival strategy the flight altitude is the same for both the lateral as the longitudinal escape maneuver. This indicates that lateral maneuvering in this case is used to gain airspeed to increase the kinetic level of the specific energy (Fig. 5b). The ground tracks (Fig. 5c) show that in the final stage of the escape maneuver the aircraft ends up flying along a wind radial. In a lateral escape maneuver this alignment takes place in the after-shear region.

The control variables, viz. the angle of attack and the bank angle, are shown in Figs. 5d and 5e. From the plot of the angle of attack it can be observed that for lateral escape maneuvers the maximum value is reached earlier. As a consequence of the long stay at the maximum value of the angle of attack during the performance strategy, a phugoid type of flight can be detected again. With respect to the bank angle Fig. 5e shows a 'wiggle' at the end of the time histories. This peculiar roll behaviour occurred in all performed optimizations, however, it is important to notice that the controls in the final part of the optimization process have virtually no impact on the actual value of the performance index.

The effect of lateral maneuvering on the windshear hazard factor is visualized in Fig. 5f. It can be readily seen that lateral maneuvering has a positive effect. Due to turning it is possible to avoid a part of the unfavorable windshear, which becomes visible in the shorter positive F-factor plateau. This plateau displays the energy drain caused by the downdraft and the tailwind of the microburst.

CLOSED-LOOP GUIDANCE TRAJECTORIES

The preceding scenarios represent microburst encounters featuring short-range forward-look windshear detection.

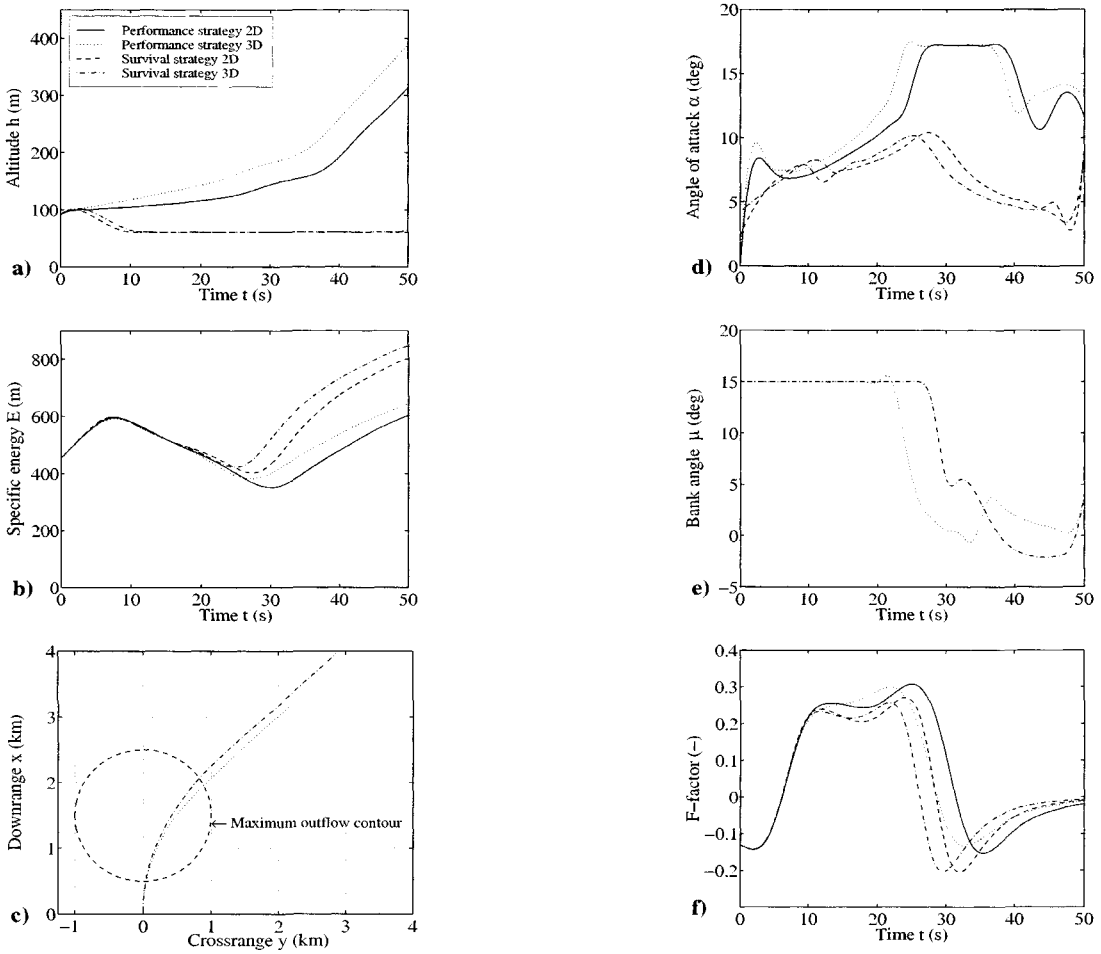

Fig. 5 Comparison of longitudinal (μ_{max} = 0°) and lateral (μ_{max} = 15°) optimal solutions.

To approximate the obtained open-loop optimal trajectories, two near-optimal closed-loop escape strategies, which rely on relatively short-range forward-look windshear detection systems, are developed. The proposed escape guidance laws have been synthesized along the lines of [9], involving nonlinear dynamic inversion (NDI) analysis. The essence of dynamic inversion is to find a nonlinear transformation of variables (via the introduction of so-called pseudo controls), through which a nonlinear system can be transformed into a linear system. Subsequently, a control law can be developed that gives the linear system the desired characteristics, after which an inverse transformation takes place to the original variables. The dynamic inversion technique is particularly useful for determining the control inputs to obtain desired outputs.

To use feedforward information in the developed closed-loop lateral guidance laws, a simulation program is set up that is capable of simulating forward-look detection by computing the wind vector and its spatial gradients at a single point located at a range r_{look} along the flight path vector. In this way it is possible to predict the F-factor based on advance wind information, in combination with the momentary aircraft state. An escape maneuver can be initiated as soon as the predicted F-factor value exceeds a specified F-factor detection threshold F_{thres}. One must realize that this is just a simplified representation of a forward-look detection system.

The take-off maneuver in the used simulation program is divided into three phases. Initially, the aircraft is assumed to be on a safe climb out (phase 1). A switch to the escape logic (phase 2) is initiated once the forward-look F-factor exceeds a threshold value ($F_{look} > F_{thres}$). This escape logic involves the horizontal and vertical guidance laws, which will be discussed in the next two sections. The switch to the last phase (phase 3) is performed if the energy drain has stopped. In this phase a climb-out is performed, which moves the aircraft away from its recovery altitude.

HORIZONTAL GUIDANCE. From the behaviour of the optimal trajectories it was concluded, that in the after shear region of a microburst the aircraft lines up with a wind radial, or in other words, the difference between the radial wind direction and the actual heading ($\chi_W - \chi$) tends to go to zero. To control this 'heading error' to zero a simple guidance law, as presented in [10], is used:

$$\mu_c = K_\mu(\chi_W - \chi), \qquad |\mu_c| \le \mu_{\max} \tag{27}$$

with the gain coefficient K_μ selected as 0.25 and where it is understood that:

$-180^\circ \le \chi \le 180^\circ$ and $-180^\circ \le \chi_w \le 180^\circ$

VERTICAL GUIDANCE. In this section two different vertical guidance strategies are presented, namely climb rate guidance and altitude guidance. Both strategies are developed to approximate the performance maintaining optimal solutions, since it was concluded that this was the safest escape strategy. The difference between the already existing vertical guidance strategies, as presented in [10], and the guidance strategies which will be described here, is the use of short-range forward-look sensing. This forward-look sensing makes it possible to anticipate a microburst encounter to some extent.

Climb rate guidance. The idea behind a climb rate guidance strategy is to design a guidance law that couples climb rate to the aircraft's specific energy in order to manage climb performance. The objective is to give the climb rate the following first-order response characteristic:

$$\dot{C} = \frac{1}{\tau}(C_c - C) \qquad \text{or} \qquad \ddot{h} = K_h(\dot{h}_c - \dot{h}) \tag{28}$$

where $C_c = \dot{h}_c$ is the desired (commanded) climb rate; and τ is a selected time constant.

Differentiation of the kinematic equation for rate of climb (Eq. (3)) gives:

$$\begin{aligned} u_c = \ddot{h} &= V\dot{\gamma}\cos\gamma + \dot{V}\sin\gamma + W_h \\ &= g\left[\sin\gamma\,\frac{T\left[1-\frac{1}{2}(\alpha+\delta)^2\right]-D}{W}\right. \\ &\left. + \cos\gamma\,\frac{L+T(\alpha+\delta)}{W}\cos\mu - 1\right] \end{aligned} \tag{29}$$

where u_c is the artificially introduced pseudo control. It can be observed that Eq. (29) relates u_c to a quadratic polynomial in α, which is the original control variable. By relating Eq. (29) to Eq. (28), the pseudo control u_c can be defined.

Assuming that the aerodynamic roll angle command has been evaluated using Eq. (27) and that the thrust T is known, the angle of attack can now be calculated from solving Eq. (29) for α.

The commanded climb rate is scheduled in terms of the aircraft's available climb performance:

$$\dot{h}_c = \dot{h}_{nom} + K_{E_1}\left[\dot{E}(t) - \dot{E}_{nom}\right] + K_{E_2}\frac{dx}{dt}\frac{\dot{E}_{pred} - \dot{E}(t)}{dx} \tag{30}$$

where dx is the forward-look distance r_{look} ; $\dot{h}_{nom}$ is the nominal climb rate; $\dot{E}_{nom}$ is the nominal energy rate; and $\dot{E}_{pred}$ is the predicted value of the energy rate at a distance r_{look} . It can be seen that Eq. (30) consists of three parts. The first part, which includes the nominal climb

rate, ensures that the aircraft is able to continue the climb out if no windshear is present ($\dot{E}(t) = \dot{E}_{pred} = \dot{E}_{nom}$). The second (feedback) part deals with the energy gain/drain if a microburst is present. If during a favorable part of the microburst the aircraft is able to gain energy, the second part of Eq. (30) will lead to a positive value, since $\dot{E}(t) > \dot{E}_{nom}$. This results in a commanded climb rate that is higher than the nominal value. On the other hand, if the aircraft flies through an unfavorable part of the microburst, a lower commanded climb rate is desirable to cope with the energy drain due to the downdraft and the horizontal wind velocities. Now, the energy drain causes a lower commanded climb rate in Eq. (30), since $\dot{E}(t) < \dot{E}_{nom}$. The third part is the feedforward part. This part allows to build up an energy buffer by lowering the commanded climb rate before the microburst penetration actually starts. To determine the aircraft state at r_{look} and thus the necessary $\dot{E}_{pred}$, the current aircraft state and the wind data at r_{look} are used.

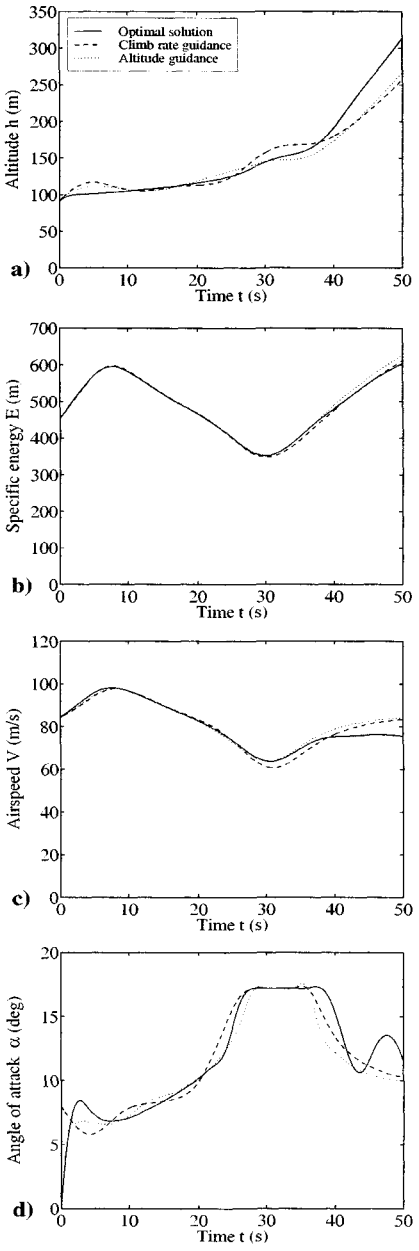

Fig. 6 Comparison of closed-loop guidance solutions with the open-loop optimal solution. Longitudinal maneuvering.

The gain factors in Eqs. (28) and (30) are selected as follows: $K_h = 0.25$; $K_{E_1} = 0.25$; $K_{E_2} = 3.75$; and dx/dt is approximated as a constant at 81 m/s.

Altitude guidance. Altitude guidance has the same objective as climb rate guidance, namely to approximate the open-loop optimal solutions. The development of the new guidance strategy is also based on NDI, only now the pseudo control in Eq. (29) is defined as a second-order response characteristic:

$$u_c = \ddot{h} = -\left(2\zeta\omega_0\dot{h} + \omega_0^2(h - h_c)\right) \tag{31}$$

where $\zeta = 0.8$ and $\omega_0 = 0.25$ have been selected. This law directs the aircraft towards the commanded altitude. Here the following commanded altitude is used:

$$h_c = h_0 + \frac{\left\{\tan(\gamma_{e_0}) + K\left[\tan(\gamma_{e_0})\right]_{pred}\right\}x}{1+K} \tag{32}$$

where h_0 is the altitude at initiation of the simulation; γ_{e_0} is the nominal absolute flight path angle; $\tan(\gamma_{e_0})_{pred}$ is the predicted value of $\tan(\gamma_{e_0})$ at a distance r_{look} ; x is the downrange; and $K = 1.25$.

The basic idea behind this commanded altitude will be described briefly. When an aircraft is on a safe climb out, it flies a prescribed trajectory. If a microburst is present, it is not possible to maintain this trajectory. The main objective than, is to closely approximate the optimal flight trajectory. From Eq. (32) it can be seen that in a windless environment the commanded altitude is equal to the optimal trajectory, because in that case the predicted value of the absolute flight path angle at a distance r_{look} is equal to the initial absolute flight path angle:

$$\left[\tan(\gamma_{e_0})\right]_{pred} = \tan(\gamma_{e_0}) \tag{33}$$

If on the other hand a microburst is detected, the forward-look term in Eq. (32) will lead to a lower value, because it is not possible to maintain the nominal flight path angle during the microburst penetration. As a result the commanded altitude is lower than in the nominal case. In this way the aircraft can anticipate on the coming microburst and build up an energy buffer.

It must be remarked that a protection switch is put in the altitude guidance simulation program, to avoid an early increase of the forward-look term. This protection switch indicates when the energy drain stops. One can imagine that when an aircraft flies through the unfavorable region of the microburst (energy drain), the forward-look system already calculates an F-factor value that is outside this unfavorable region. This may result in a commanded altitude, which is too optimistic. The protection switch holds the last commanded (low) forward-look term until the actual energy drain has stopped. Once the energy drain has stopped climb rate guidance is used instead of altitude guidance to initiate a safe recovery (phase 3).

SIMULATED GUIDANCE SOLUTIONS. Throughout the simulation an F-factor detection threshold value F_{thres} = 0.04 and a forward-look distance r_{look} = 500 m, in combination with the proposed climb rate guidance and altitude guidance laws are used to approximate the optimal solutions. The same scenario (initial aircraft state, control constraints and microburst parameters) is used as in the open-loop optimization study.

Longitudinal escape maneuvers. From Fig 6.a it can be seen that the two guidance strategies closely approximate the optimal trajectory. Only at the end the guidance strategies deviate from the optimal solution, which is a result of the recovery strategy in the after shear region of the microburst (phase 3). In this recovery strategy a lower climb rate is commanded in relation to the optimal trajectory. However, it must be mentioned that in general an optimal trajectory obtained with a higher reference climb rate only differs from the other trajectories in the after shear region of a microburst. It can also be observed that the climb rate guidance trajectory tries to increase altitude after approximately 26 seconds, but decreases again after 32 seconds. This is an effect of the forward-look part of Eq. (30). After 26 seconds the forward-look part already calculates a positive energy rate, while the actual energy rate is still negative. As a consequence a climb rate is commanded, which can not be reached yet. This implies that the third part of Eq. (30) plays a larger role than the second part. Changing the gain factors can solve this problem, but the current gain factors provide a good overall performance. In the altitude guidance strategy the protection switch suppresses this behaviour. The last commanded forward-look part in Eq. (32) is maintained if the energy drain is still present. Applying this switch to the climb rate guidance increased the performance in this case, but the overall performance decreased again. Therefore the protection switch is not applied in the climb rate guidance strategy.

Figure 6.b shows the specific energy. It can be observed that due to the forward-look parts in the guidance

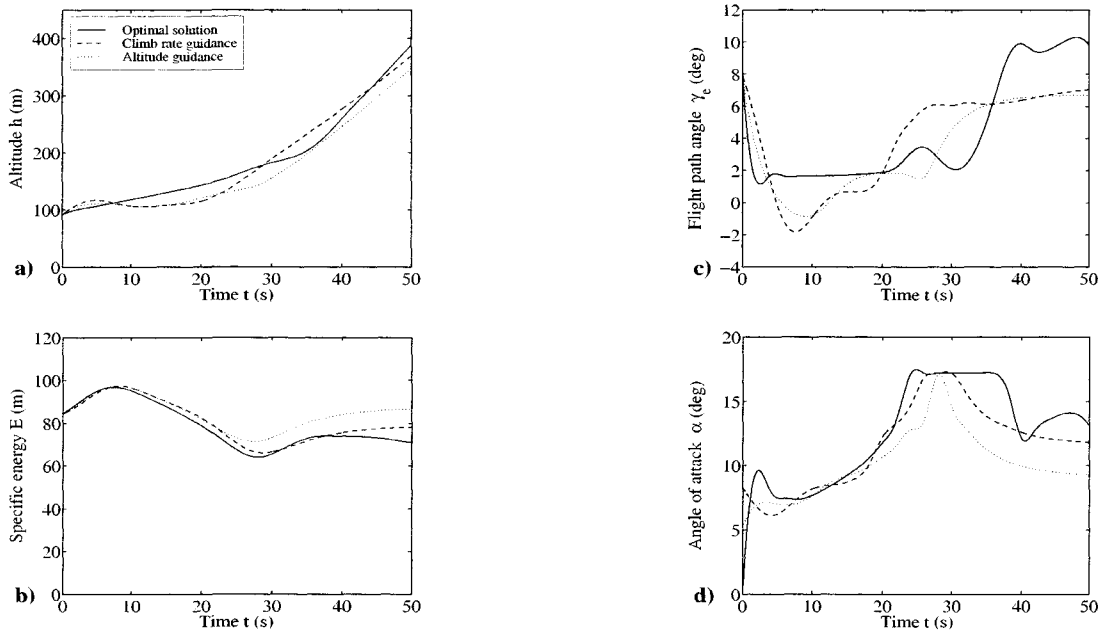

Fig. 7 Comparison of the simulated guidance solutions with the optimal solution. Lateral maneuvering (μ_{max} = 15°).

strategies an energy buffer is build up. This energy buffer is in both guidance strategies the result of a lower initial climb rate in order to gain airspeed (see Fig. 6.c).

The low minimum airspeed in the climb rate guidance strategy can be explained by the high altitude at that moment. Since the angle of attack is already at its maximum value (see Fig. 6.d), airspeed is exchanged in order to increase the altitude. The minimum specific energy, however, is in all cases about the same.

Lateral escape maneuvers. Using the same gain factors as in the longitudinal case, the guidance strategies show again good altitude performance (Fig. 7.a). It can be seen that during the unfavorable region both the guidance strategies impose a lower commanded climb rate or climb angle in order to gain airspeed and, consequently, specific energy (Fig. 7.b). Due to the lateral maneuvering, the climb rate guidance strategy does not experience the negative influence of the forward-look part, as described in the longitudinal escape maneuver. The lower altitude makes it even possible to go to the nominal climb rate much earlier than in the optimal trajectory. This can also be seen in Fig. 7.c, where the nominal absolute flight path angle is reached in a very early stage of the escape maneuver. As a consequence the reached final altitude does not differ much from the optimal final altitude. The altitude guidance strategy on the other hand, maintains the lower altitude longer due to the protection, which is put in the simulation program to prevent that a high climb angle is initiated before the energy drain has stopped. Therefore the final altitude in this case is lower. Due to high airspeeds in the unfavorable region of the microburst, the aircraft does not fly at its maximum angle of attack for a long time, as is the case during the optimal trajectory (see Fig. 7.d). The overall effect of the low altitude and the high airspeed is a high minimum and final specific energy.

Influence of the forward-look distance. One can imagine that the forward-look distance r_{look} plays an important role in the proposed guidance strategies. The short-range forward-look results of the preceding sections have already demonstrated that the potential performance benefits of forward-look sensing are sufficient to approximate the optimal solutions. This indicates that the forward-look distance is a very important parameter in the proposed guidance strategies. Therefore, three different forward-look distances are used in the climb rate guidance strategy, to study the effect on flight performance.

For simulation of the lateral escape maneuvers, the microburst is placed at 1750 m from the starting point without lateral displacement. The used forward-look distances are 250 m, 500 m and 750 m. This implies that with a r_{look} of 750 m the escape maneuver is initiated immediately at the beginning of the simulation.

An aircraft, which contains forward-look equipment with a low r_{look} value, will fly the normal climb out until the threshold F-factor is passed. After passing this threshold F-factor the escape maneuver will be initiated. This behaviour can be clearly seen in Fig. 8.a. The simulation with a r_{look} value of 250 m initiates the escape maneuver just after having covered a distance of approximately 550 m from the origin. Until this time the

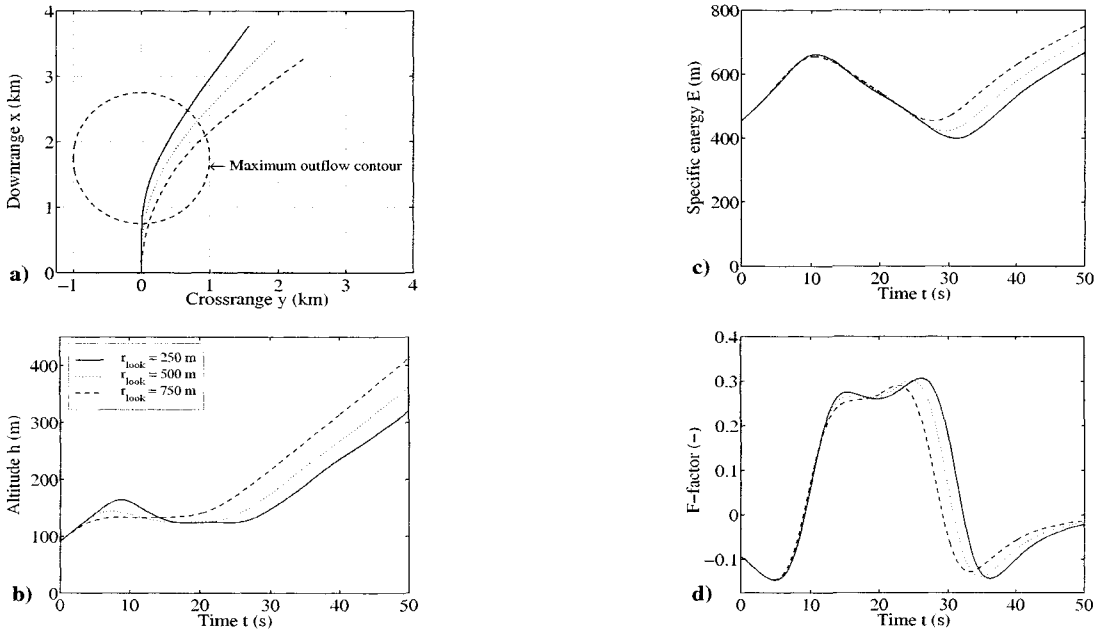

Fig. 8 Comparison of closed-loop guidance solutions for various values of r_{look}. Lateral maneuvering (μ_{max} = 15°).

aircraft flies a normal climb out.

Figure 8.b shows that the late microburst detection has a negative influence on flight altitude. If an aircraft penetrates the microburst at a high altitude, a high downdraft will be experienced which in turn decreases the altitude. A high r_{look} value however, prevents that initially the altitude is increased too much. This has two advantages, namely a low experienced downdraft, since the aircraft keeps flying on a low altitude, and the possibility to build up an energy buffer by increasing the airspeed. From Fig. 8.b it can be seen that in the simulation with a low r_{look} value initially a higher altitude is reached (at the expense of airspeed), because the microburst is detected later. In the simulation with a high r_{look} value however, the altitude is kept almost constant during the favorable first region of the microburst in order to gain airspeed and build up an energy buffer (Fig. 8.c). Since the minimum reached altitude is almost the same in all three cases, it can be concluded that the current selection of the gain factors is a good compromise between performance and robustness.

Figure 8.d shows that due to the forward-look equipment the escape is commenced when the aircraft is still in the region of increasing headwind ($F < 0$). A negative F-factor in combination with the full throttle explains the observed initial energy increase (Fig. 8.c).

From the groundtracks (Fig. 8.a) it becomes clear that the early initiated escape maneuver due to the high r_{look} value reduces the extent of the high shear region that is traversed.

CONCLUSIONS

In this paper take-off maneuvers in the presence of windshear are considered with reference to flight in the vertical and horizontal plane. Attention is focussed on the open-loop optimization of two escape strategies, viz. a performance maintaining strategy and a survival strategy, in combination with early microburst detection. Also, a study on the development of closed-loop guidance strategies featuring short-range forward-look detection, which closely approximate the open-loop optimal solutions, has been presented.

Comparison of the two open-loop optimal escape strategies made clear that that the performance maintaining strategy in a severe microburst environment eventually evolved into a survival strategy, which indicated that the performance maintaining strategy is probably the safest strategy. Furthermore, the introduction of lateral maneuvering during the take-off maneuver showed that turning the aircraft away from the microburst core led to a significant improvement of the flight performance, in the performance maintaining strategy as well as the survival strategy. This improvement of flight performance is a result of the positional advantage relative to the microburst core in the case of lateral maneuvering, in comparison to straight flight.

The simulation results showed that the employed climb rate and altitude guidance strategies were able to closely approximate the optimal trajectories, in both longitudinal and lateral escape maneuvers, and that the current selection of the gain factors is a good compromise between performance and robustness. It can thus be concluded, that by applying advance warning systems flight performance can be improved significantly. However, it must be realized that the current simulation results are obtained with a simplified representation of forward-look detection systems. It is clear that for practically use of the proposed guidance strategies a more appropriate representation of forward-look detection systems is required.

REFERENCES

1. Bowles, R.L., "*Reducing Windshear Risk Through Airborne Systems Technology*", Proceedings of the 17th ICAS, Part II, pp. 1603-1630, Stockholm, Sweden, 1990.
2. Miele, A., Wang, T. and Melvin, W.W., *"Optimal Take-Off Trajectories in the Presence of Windshear"*, Journal of Optimization Theory and Applications, Vol.49, No.1, April 1986, pp. 1-45.
3. Bryson, A.E. and Zhao, Y., *"Optimal Paths Through Downbursts"*, Journal of Guidance, Control and Dynamics, Vol. 13, No. 5, Sept.-Oct. 1990, pp. 813-818.
4. Psiaki, M.L. and Stengel, R.F., *"Optimal Flight Paths Through Microburst Wind Profiles"*, Journal of Aircraft, Vol. 23, No. 8, Aug. 1986, pp. 629-635.
5. Visser, H.G., *"Optimal Lateral-Escape Maneuvers for Microburst Encounters During Final Approach"*, Journal of Guidance, Control and Dynamics, Vol. 17, No. 6, Nov.-Dec. 1994, pp. 1234-1240.
6. Soesman, J.L., *"Control of Aircraft Through Windshear After Take-Off"*, NLR TR 90116 L, 1990.
7. Visser, H.G., *"A Minimax Optimal Control Analysis of Lateral Escape Maneuvers for Microburst Encounters"*, Journal of Guidance, Control and Dynamics, Vol. 20, No. 2, 1997, pp. 370-376.
8. Hargraves, C.R. and Paris, S.W., *"Direct Trajectory Optimization Using Nonlinear Programming and Collocation"*, Journal of Guidance, Control and Dynamics, Vol. 10, No.4, July-Aug. 1987, pp. 338-342.
9. Mulgund, S.S. and Stengel R.F., *"Aircraft Flight Control in Wind Shear Using Sequential Dynamic Inversion"*, Journal of Guidance, Control and Dynamics, Vol. 18, No. 5, Sept.-Oct. 1995, pp. 1084-1091.
10. Visser, H.G., *"Lateral Escape Guidance Strategies for Microburst Windshear Encounters"*, Journal of Aircraft, Vol. 34, No. 4, July-August 1997, pp. 514-521.